



# High-resolution spectroscopy (XPS, $^1\text{H}$ MAS solid-state NMR) and DFT investigations into Ti-modified Phillips $\text{CrO}_x/\text{SiO}_2$ catalysts

Ruihua Cheng<sup>a</sup>, Chen Xu<sup>a</sup>, Zhen Liu<sup>a</sup>, Qi Dong<sup>a</sup>, Xuelian He<sup>a</sup>, Yuwei Fang<sup>b</sup>, Minoru Terano<sup>b</sup>, Yatao Hu<sup>c</sup>, Thomas J. Pullukat<sup>c</sup>, Boping Liu<sup>a,\*</sup>

<sup>a</sup> State Key Laboratory of Chemical Engineering, East China University of Science and Technology, Meilong Road 130, Shanghai 200237, PR China

<sup>b</sup> School of Materials Science, Japan Advanced Institute of Science and Technology, 1-1 Asahidai, Nomi, Ishikawa 923-1292, Japan

<sup>c</sup> Research and Development Center, The PQ Corporation, 280 Cedar Grove Road, Conshohocken, PA 19428-2240, USA

## ARTICLE INFO

### Article history:

Received 2 November 2009

Revised 6 May 2010

Accepted 11 May 2010

Available online 16 June 2010

### Keywords:

Phillips  $\text{CrO}_x/\text{SiO}_2$  catalyst

Ti-modification

X-ray photoelectron spectroscopy

$^1\text{H}$  magic-angle-spin solid-state nuclear

magnetic resonance

Density functional theory

## ABSTRACT

Ti-modified Phillips catalyst is a most important industrial catalyst widely used in ethylene polymerization, but the mechanism still remains mysterious. In this work, Ti-modified Phillips catalysts were characterized by high-resolution X-ray photoelectron spectroscopy (XPS) and  $^1\text{H}$  magic-angle-spin solid-state nuclear magnetic resonance ( $^1\text{H}$  MAS solid-state NMR) combined with density functional investigations into the effects of Ti-modification on promotion of polymerization activity and regulation of microstructures of the polymer chains. XPS data revealed Ti-modification caused increase in electron-deficiency and photo-stability of the surface chromate species.  $^1\text{H}$  NMR provided the first direct evidence of surface residual Ti–OH groups. Modeling results rationalized well the effects of Ti-modification on promotion of polymerization activity, extension of molecular weight distribution (MWD) to lower MW region, improvement of the distribution of inserted co-monomer and enhancement of 2,1-insertion in regioselectivity of Phillips catalysts. It was the first time the Ti-modification on Phillips catalysts were theoretically elucidated.

© 2010 Elsevier Inc. All rights reserved.

## 1. Introduction

Phillips catalyst, with highly dispersed chromium oxide covalently anchored on silica gel surface, is one of the most important industrial olefin polymerization catalysts and nowadays is roughly producing 10 million tons of high-density polyethylene (HDPE) about 50% of the world HDPE market [1–3]. Its HDPE products are featuring with ultra-broad molecular weight distribution (MWD), long-chain branches, and specially applicable for blow molding products like hollow containers and pipes. In the last decades, the applications from exclusive Phillips HDPE products for the gasoline tanks of the automobile industry and ultra large size plastic pipes and containers make a successively increasing market demanding.

Due to its great commercial importance, the Phillips catalyst has been intensively studied since its discovery in the early 1950s. Despite the great research efforts, the academic progresses about this catalyst are lagging far behind its successful commercial applications. Most importantly, the nature of the active sites and the exact initiation/polymerization mechanisms on the Phillips catalyst still remain controversial [1–3]. The difficulties for basic

studies on this catalyst system mainly derived from the low percentage of active Cr species, the complexity of heterogeneous catalyst system, the multiple valence states of Cr, the fast encapsulation of active sites by produced polymer, and the very fast polymerization rate.

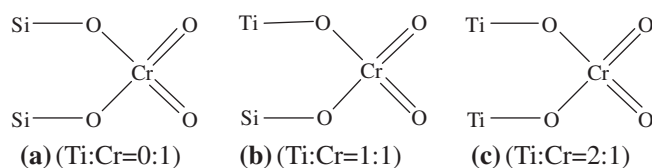
Phillips catalyst is usually prepared by a simple impregnation of porous silica gel support with aqueous solution of Cr(III) acetate and a subsequent drying followed by an important calcination process in dry air at a certain temperature between 500 °C and 900 °C to obtain a calcined catalyst stored in  $\text{N}_2$  atmosphere [1,3]. During the calcination process, the Cr(III) acetate decomposed into  $\text{CrO}_3$  followed by esterification reaction with the surface hydroxyl groups on silica gel resulting in the formation of chromate species including monochromate, dichromate, or even polychromate. The most unique feature of Phillips catalyst is that the calcined catalyst could be directly activated by ethylene monomer for ethylene polymerization without using any organometal cocatalysts. The performance of the calcined Phillips catalyst is known to be greatly dependent on the history of calcination process in terms of either physical or chemical modifications. During the past several decades, a series of important chemically modified Phillips catalysts have been successfully developed including the modifications of the silica gel support by titanium, aluminum, fluorine, etc. [1–3]. Ti-modified Phillips catalyst, which was first developed by Phillips

\* Corresponding author. Fax: +86 21 64253627.

E-mail address: [boping@ecust.edu.cn](mailto:boping@ecust.edu.cn) (B. Liu).

Petroleum Co., in the late 1960s, has been becoming a most important industrial catalyst widely used in the Phillips ethylene polymerization processes [2–10]. The Ti-modification could not only efficiently improve the catalyst activity but also provide an important method for regulation of the molecular weight (MW), MWD, and inserted co-monomer distribution in polymer products, as the Phillips catalyst is not sensitive to chain transfer with hydrogen as Ziegler–Natta and metallocene catalysts.

In spite of the commercial importance, Ti-modified Phillips catalysts have not been fully investigated in the literature. In general, Ti-modification in terms of titania incorporation to Phillips catalyst could be fabricated by either co-gel or surface impregnation method. The co-gel method incorporated titania by adding titanium salts like  $\text{TiCl}_4$  into the silicate solution for the sol-gel process and led to the dispersion of titania in the bulk of the synthesized silica gel support, while the surface impregnation method incorporated titania on the surface through simple impregnation of titanium ester onto silica gel support followed by calcination at high temperatures [2–7]. Nowadays, Ti-modified Phillips catalysts by both methods are applied in commercial polyethylene processes for production of HDPE with only slight difference in polymer properties [2]. According to Weckhuysen and coworkers [11], the surface titania species over silica gel enhanced the concentration of surface polychromate species leading to comparable amount of surface monochromate and polychromate species based on Raman characterization. McDaniel et al. [2] reported that Ti-modification could induce decrease in thermal stability of Phillips catalysts resulting in the occurrence of earlier catalyst sintering at lower calcination temperatures. Thus, an optimal titania loading for commercial Ti-modified Phillips catalyst was usually less than 5 wt.% Ti. Generally, Ti-modification could play the following four most important roles in the performances of Phillips catalysts [2,3,10]. (i) Ti-modification could increase the catalytic polymerization activity in terms of the Ti-promotion effect with a shorter induction period and higher maximum polymerization rate. (ii) Ti-modification could broaden the MWD of the polymer product to low MW region and thus decrease the average MW. As observed by McDaniel, with the gradual increasing of the Ti-loading, the MWD gradually extended to lower MW part without any variation at the high MW end. (iii) Ti-modification could obviously decrease the incorporation of co-monomer (1-hexene or 1-butene) in the low MW region and increase the density of the polyethylene. Such variation of the distribution of inserted co-monomer in polyethylene chain significantly improved the mechanical properties of the final products. As declared by McDaniel [2], there existed two seemingly contradictory points as follows. One was that Ti-modified Cr active sites preferred to produce low MW polyethylene with low co-monomer incorporation, while low MW polyethylene made by Cr active sites without Ti-modification showed high co-monomer incorporation. The other was that the chain transfer response to co-monomer of Ti-modified Phillips catalyst was much greater than that of Ti-free Phillips catalyst, while the product of Ti-modified Phillips catalyst incorporated much less co-monomer contents. (iv) Ti-modification could obviously increase the trans-internal unsaturation chain ends. Based on this experimental fact, McDaniel suggested that 2,1-insertion versus 1,2-insertion might be enhanced during ethylene copolymerization with  $\alpha$ -olefin indicative of a variation in regioselectivity of the catalyst. In summary, the mechanistic understanding on the four aforementioned most important roles of Ti-modification for Phillips catalysts has not been achieved yet. Accordingly, these unique effects should be derived from the change of active site distribution through possible formation of new active Cr species related to Ti-modification. As shown in Scheme 1, Pullukat and coworkers first proposed a site model of monochromate species directly linked to the surface



**Scheme 1.** Proposed formation of Ti–O–Cr bridges on Ti-modified Phillips catalyst in Ref. [7].

titania through two Cr–O–Ti bridges [7,10]. McDaniel et al. [2] proposed similar site model based on experimental investigations into a Ti-modified Phillips catalyst prepared from  $\text{CrO}_2\text{Cl}_2$ . Moreover, the linkage of chromate species onto surface titania through Cr–O–Ti bridge was also indirectly confirmed by spectroscopic characterizations with diffuse reflectance spectroscopy (DRS), electron paramagnetic resonance (EPR), and temperature-programmed reduction (TPR) [7,12]. Based on the previous understanding in the literature, detailed mechanistic investigations into Ti-modified Phillips catalysts are in high demand for further progress in this important field.

Among various surface analytical techniques, high-resolution X-ray photoelectron spectroscopy (XPS) with high surface sensitivity (typical sampling depths of 1–2 nm) is one of the most powerful methods for both quantitative and qualitative characterizations of surface chromate species over Phillips catalyst with relatively low Cr loading [10,13–17]. The first XPS study on Ti-modified Phillips catalyst was reported by Pullukat and coworkers [13] in 1980. They found the binding energy (BE) of Cr  $2p_{3/2}$  for chromate species decreased from 579.6 eV to 578.0 eV after Ti-modification suggesting the increase in electron density and decrease in oxidizing capacity for the chromate species. This means Ti-modified chromate species became much more difficult to be reduced by ethylene monomer, which was contradictory to the experimental evidence that Ti-modification facilitated the reduction of chromate species featuring with shorter induction period and higher polymerization rate. This discrepancy probably originated from the following reasons. First, improper reference peak C 1s = 285.0 eV from carbon contamination was selected for their correction of charging effect during XPS measurement. We [17] have shown that reference peak C 1s = 285.0 eV from carbon contamination might cause significant error for BE value due to the different carbon contamination for different samples, and the Si 2p peak at 103.3 eV from silica gel support was ideal for the charging effect corrections. Secondly, the resolution of the XPS instrument was not high enough to get accurate data for catalysts with low Cr loading. The second XPS study on Ti-modified Phillips catalyst was reported by McDaniel et al. [10] in 1983. They found that the Ti species tended to migrate from the bulk phase of silica gel support to its surface during calcination for co-gel type Ti-modified Phillips catalysts through measuring the intensity ratio of the Ti 2p and Si 2p peaks. The BE values of the chromate species with and without Ti-modification were not measured. After more than 30 years of technical development, the XPS instrument has been improved significantly with high resolution for not only qualitative but also precise quantitative characterization of surface chromate species, the precursor of the active sites, for industrial Phillips catalysts with relatively low Cr loading. Therefore, much deeper mechanistic insight into the Ti-modified Phillips catalyst through XPS method becomes possible and is urgently needed. Following our previous series of investigations into Phillips catalysts by high-resolution XPS method [16,17], in this work the BE value and the full width at half maximum (FWHM) of Cr  $2p_{3/2}$  peak for the surface chromate species with or without Ti-modification were monitored in terms of catalyst preparation methods, calcination temperatures, and Ti contents. We [16,17] have previously found that the XPS data obtained within 10 min

acquisition of high-resolution scanning could reflect the original physico-chemical nature of surface chromate species with negligible photo-reduction. However, longer XPS acquisition time (over 10 min) could induce photo-reduction of some labile hexa-valent chromate species into tri-valent Cr species due to the soft X-ray irradiation [14,16–18]. Our more recent report [16] revealed an interesting relationship between the photo-stability of the surface chromate species during XPS measurements and the polymerization activity for Phillips catalysts calcined at different temperatures. It was found the photo-stability of the chromate species on Phillips catalysts increased with the increasing calcination temperatures (200–800 °C), which was corresponding to simultaneous increase in oxidizing capacity of chromate species and polymerization activity as well. Although the mechanism of the aforementioned correlation between the photo-stability and oxidizing capacity of chromate species and polymerization activity was still unclear, the XPS characterization in terms of photo-stability could be utilized in this work for the precise investigations into the effects of Ti-modification over Phillips catalysts.

During the last decade, computational molecular simulation based on density functional theory (DFT) is becoming more and more important and powerful to get molecular-level insight into Cr active site and its polymerization mechanism of Phillips catalyst. Espelid and Borge [19–21] have studied on three possible polymerization mechanisms involving Cossee mechanism, carbene mechanism, and metallacycle mechanism on Phillips catalyst by DFT method using mononuclear, dinuclear disiloxanochromium(II) catalyst models, and found that the metallacyclic initiation presented the lowest energy barrier. Very recently, Scott and coworkers [22] confirmed the mononuclear disiloxanochromium(II) 6-ring model might be the most plausible active site, which showed much higher polymerization activity than that of the mononuclear trisiloxanochromium(II) 8-ring model through DFT method combined with experiments. Damin et al. [23] studied on the molecular modeling of the mononuclear disiloxanochromium(II) model adsorbed with probe molecules of CO and N<sub>2</sub> and found that more accurate simulated IR spectra compared to experimental IR data were obtained with increasing the percentage of Hartree–Fock exchange in the hybrid density functional. Ziegler and Schmid [24] studied the ethylene polymerization mechanisms by DFT method over a neutral disiloxanochromium(IV)–carbene model and found that a transformation from the Cr–carbene into a cationic Cr–C site followed by the Cossee type chain propagation might be most plausible. By the combination of DFT and paired interacting orbitals (PIO), we previously studied the intermolecular orbital interactions between ethylene monomer and various monochromate models of Phillips catalyst in terms of the effects of supporting of chromium compounds [25] and the fluorination of the silica gel support surface [26]. More recently, our DFT and PIO studies on the effects of oxidation state and surface hydroxyl on the polymerization activity of various disiloxanomolybdenum–methyl model catalysts disclosed that divalent Mo<sup>2+</sup> might be the most plausible active site for silica gel supported-MoO<sub>x</sub> ethylene polymerization catalysts [27]. However, up to now, no molecular modeling study focusing on the effects of Ti-modification for Phillips catalyst has been reported.

In this work, the effects of Ti-modification on Phillips catalysts with respect to its promotion of polymerization activity, extension of MWD to lower MW region, improvement of the distribution of the inserted co-monomer, and the enhancement of 2,1-insertion in regioselectivity were systematically investigated by DFT method combined with high-resolution XPS and <sup>1</sup>H magic-angle-spin solid-state nuclear magnetic resonance (<sup>1</sup>H MAS solid-state NMR) characterization. As for the experiments, the oxidation state and photo-stability of the surface Cr species on Ti-modified Phillips catalysts with dependence on the XPS acquisition time was also

characterized in order to correlate with its electronic properties and polymerization behavior as well. High-resolution <sup>1</sup>H MAS solid-state NMR method was applied to confirm the existence of surface residual Ti–OH groups on Ti-modified Phillips catalysts, which verified the reliability of the active site models constructed for computational molecular modeling. Much deeper mechanistic understanding on the effects of Ti-modification over Phillips catalysts was demonstrated.

## 2. Experimental and computational

### 2.1. Catalysts

In this work, eight Phillips catalysts (named as **Ph-1** to **Ph-8**) with or without Ti-modification stored within small N<sub>2</sub>-filled and sealed stainless steel containers were all donated from PQ Corp., USA. Among them, seven catalysts from **Ph-2** to **Ph-8** including five Ti-modified catalysts (**Ph-2**, **Ph-4**, **Ph-5**, **Ph-7**, and **Ph-8**) made by surface impregnation method and two catalysts (**Ph-3** and **Ph-6**) without Ti-modification were commercial ethylene polymerization catalysts produced by PQ Corp. The chromium content for each catalyst sample was ca. 1 wt.% Cr. The **Ph-1** containing 2.22 wt.% Ti was a co-gel type Ti-modified Phillips catalyst prepared according to Dietz's patent [6]. The specific preparation procedure for **Ph-1** is shown as follows. First, after 43 g sulfuric acid (95%) was mixed with 4.25 g (2.5 ml) TiCl<sub>4</sub>, water was added to reach a total volume about 270 mL. Then, 255 g sodium silicate solution (Na<sub>2</sub>O<sub>3</sub>·2SiO<sub>2</sub>, 38 wt.%,  $\rho = 1.39 \text{ g mL}^{-1}$ ) was added and mixed at 16.2 °C. Gelation occurred at pH = 6 and aged for about 4 h at 90.0 °C. The gel was washed, dried, and then impregnated with a chromium acetylacetonate in ethyl acetate followed by drying at 150 °C for 2 h under vacuum. Finally, 8 g dried sample was activated at 593 °C for 5 h within a 1-in.-diameter fluidized quartz tube reactor. The temperature of the whole calcination was programmed and linearly increased to 593 °C at 2 °C min<sup>-1</sup>. Fluidizing gas media with a flow rate of 300 mL min<sup>-1</sup> was changed from N<sub>2</sub> into dry air when temperature reached 300 °C. During the cooling stage, dry air was switched back to N<sub>2</sub> at 100 °C for purging the catalyst for 1 h followed by transfer into a storage vessel. As for the industrial catalysts (**Ph-2** to **Ph-8**) donated from PQ Corp. [28], the detailed catalyst preparation procedures would not be given herein due to the confidential reason, and only a simplified introduction of the commercial Phillips catalyst prepared by PQ Corp. was shown as follows. Grade MS-3050 silica gel with BET surface area of 480–550 m<sup>2</sup> g<sup>-1</sup>, pore volumes of 3.0 mL g<sup>-1</sup>, average pore diameter of 24 nm, average particle size of 90  $\mu\text{m}$  made by PQ Corp. was pre-dried at 170 °C to remove the physically adsorbed water and used as support. For the Ti-modified catalysts made from surface impregnation method, titanium isopropoxide was dissolved in dry *n*-heptane to impregnate onto the pre-dried silica gel support followed by drying at 250 °C for 2 h in N<sub>2</sub>. And then, the obtained samples were further impregnated with a methanolic chromium acetate solution followed by drying at 150 °C for 2 h in N<sub>2</sub>. Hereafter, the following preparation procedures were similar to that of the **Ph-1** catalyst except the final calcination temperatures. Here, the catalysts with different final calcination temperatures and Ti contents were referred to as **Ph-2** (593 °C), **Ph-4** (650 °C), and **Ph-7** (820 °C) with 2.38 wt.% Ti-loading, and **Ph-5** (650 °C), and **Ph-8** (820 °C) with 3.45 wt.% Ti-loading. Two Ti-free catalysts **Ph-3** (650 °C) and **Ph-6** (820 °C) were prepared similar to the Ti-modified catalysts by surface impregnation method skipping the impregnation of Ti compound. The BET surface areas and pore volumes of all the catalysts were measured at –196 °C using N<sub>2</sub> after evacuating the catalysts at 300 °C for 1 h. The chemical compositions (Ti and Cr loading) and textural properties including BET sur-

face area, pore volume, and average pore diameter of the catalysts are listed in Table 1.

## 2.2. XPS characterization

All the catalyst samples were characterized by high-resolution XPS method. Details concerning the XPS measurements could be found in our previous reports [16,17]. Only a simplified introduction was given here. XPS data were obtained on a Physical Electronics Perkin-Elmer Model Phi-5600 ESCA spectrometer equipped with a hemispherical electron analyzer working in the constant pass energy mode. A monochromated Al K $\alpha$  radiation (1486.6 eV) operated at 300 W was used as the X-ray source. Each sample was embedded on a conductive copper tape to form a sample disc in a diameter of 5 mm and fixed on a sample holder. The sample holder was then put into the vacuum transfer vessel (Phi Model 04-110, Perkin-Elmer Co., Ltd.), which can be connected to the sample introduction chamber on the XPS instrument for sample transfer without atmospheric exposure. The aforementioned procedures were carried out in a glove box, which had been purged overnight with nitrogen gas in advance. The prepared sample was degassed in the introduction chamber to  $10^{-7}$  Torr before entering the main chamber, where the pressure was kept below  $3 \times 10^{-9}$  torr during XPS data acquisitions. First, low resolution survey scan between 0 and 1000 eV was carried out on each sample within 2 min for a preliminary survey of all surface elements. Then, high-resolution XPS scan measurements for Cr 2p, Si 2p regions of each sample were performed within 10 min, 30 min, and 2 h. A neutralizer was used to reduce the charging effect to obtain a better signal to noise ratio. The XPS data obtained within 10 min acquisition could reflect the original physico-chemical nature of surface chromate species with negligible photo-reduction. The dependence of photo-stability of the chromate species on the XPS acquisition time (from 10 min to 2 h) was investigated to correlate with its electronic property and the catalyst polymerization behavior [14,16–18]. All binding energies (BE) were referenced to the Si 2p peak of silica gel at 103.3 eV for the charging effect correction. Multiplet fittings of the Cr 2p XPS curves by the Gaussian–Lorentzian method were carried out to determine the mixed states of valences in all the samples. The fitting for each curve was repeated for several times to ensure a reproducible result.

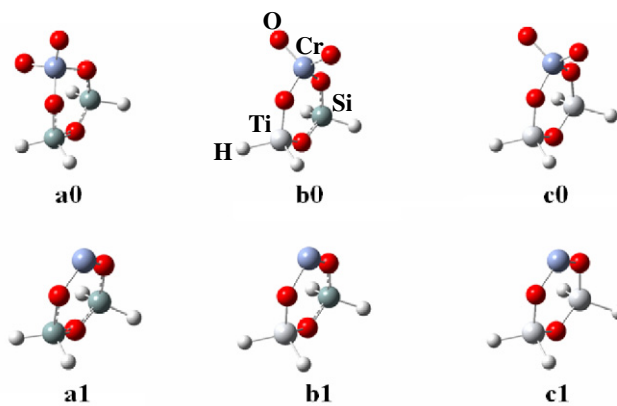
## 2.3. Solid-state NMR characterization

The six catalyst samples (**Ph-3** to **Ph-8**) were characterized by high-resolution  $^1\text{H}$  MAS solid-state NMR method at room temperature. A Varian UNITY-400 spectrometer with a Varian Room Temperature/Cross Polarization Magic Angle Spin (RT/CP MAS) probe operating at 400.47 MHz was used. Each sample (ca. 80 mg) was put and pressed tightly into a 7-mm zirconia rotor under  $\text{N}_2$  atmosphere in a glove box, which had been purged by  $\text{N}_2$  overnight before sample setting. The  $^1\text{H}$  MAS solid-state NMR spectra were

obtained with a  $30^\circ$  pulse of 3  $\mu\text{s}$ , a relaxation delay of 1 s and total 10 min acquisition time for each sample at a rotating speed of ca. 3 kHz. The spectrum of each sample was referenced to the  $^1\text{H}$  NMR spectrum of the external reference tetramethylsilane (TMS) at 0 ppm.

## 2.4. Theoretical method

All the DFT calculations were done with the Gaussian 03 software package [29]. The calculations were based on the nonlocal three-parameter UB3LYP hybrid DFT method, which was named as Becke's gradient-corrected exchange-correlation density function [30], and combining with Lee, Yang, and Parr's nonlocal correlation [31]. The LANL2DZ (Los Alamos National Laboratory second Double-Zeta) basis set [32] with relativistic effective core potential (RECP) of Hay and Wadt was used for Cr and Ti, and the 6-31G(d, p) basis set was used for the rest atoms including C, H, O, and Si. The stationary structures were optimized without any symmetry constraints and frequency calculations at the same harmonic frequencies. All energies reported referred to Gibbs free energy corrections to the total electronic energies at 298.15 K. Each reactant and product pair with minimum Gibbs free energy was used to search for the transition state, which was verified by intrinsic reaction coordinate (IRC) calculations ensuring that each transition state was directly connected to the involved reactant and product geometries [33]. Frequency calculations were all carried out to ensure that all the stationary points (reactant and product) possessed no imaginary vibrations and each transition state possessed only one imaginary vibration. The Mulliken charge of chromium atom was also calculated by Gaussian 03 program for analysis of the charge distribution on each center.



**Scheme 2.** Models for Cr(VI) sites (**a0** for Ti:Cr = 0:1, **b0** for Ti:Cr = 1:1, **c0** for Ti:Cr = 2:1) and Cr(II) sites (**a1** for Ti:Cr = 0:1, **b1** for Ti:Cr = 1:1, **c1** for Ti:Cr = 2:1) for Phillips catalyst.

**Table 1**  
Physical properties of Phillips catalysts donated from PQ Corporation.

Cat.	Type	Temp. ( $^\circ\text{C}$ )	$S_{\text{BET}}$ ( $\text{m}^2 \text{g}^{-1}$ )	$P_{\text{Vol}}$ ( $\text{mL g}^{-1}$ )	$P_{\text{Diam}}$ (nm)	Cr (wt.%)	Ti (wt.%)
<b>Ph-1</b>	Co-gel	593	502	2.52	20.0	0.9	2.22
<b>Ph-2</b>	S.I. <sup>a</sup>	593	503	2.33	18.5	1.0	2.38
<b>Ph-3</b>	–	650	505	2.34	18.6	1.0	0.00
<b>Ph-4</b>	S.I. <sup>a</sup>	650	494	2.22	18.0	1.1	2.38
<b>Ph-5</b>	S.I. <sup>a</sup>	650	499	2.17	17.4	1.1	3.45
<b>Ph-6</b>	–	820	505	2.34	18.6	1.0	0.00
<b>Ph-7</b>	S.I. <sup>a</sup>	820	494	2.22	18.0	1.1	2.38
<b>Ph-8</b>	S.I. <sup>a</sup>	820	499	2.17	17.4	1.1	3.45

<sup>a</sup> Titania was introduced by surface impregnation method.



For our theoretical DFT calculations, six mononuclear chromium cluster models including three hexa-valent chromate sites (**a0**, **b0**, **c0**) and three divalent Cr sites (**a1**, **b1**, **c1**) were utilized to mimic various Ti-modification environments on Phillips catalyst surface (shown in Scheme 2). Among these models, **a0** and **a1** were mononuclear disiloxanochromium(VI) model and mononuclear disiloxanochromium(II) model, respectively, which were most popularly accepted in the literature [19,22,23]. Models **b0** and **b1** represented Ti-modified Cr(VI) and Cr(II) catalysts, respectively, with a Ti/Cr atomic ratio of 1:1. Models **c0** and **c1** represented Ti-modified Cr(VI) and Cr(II) catalysts, respectively, with a Ti/Cr atomic ratio of 2:1. All the Ti-modified models have been previously proposed by Marsden [7], Pullukat [13], and McDaniel [2,10].

### 3. Results and discussion

#### 3.1. Experimental study of effects of preparation methods

The catalytic properties of Phillips catalysts are strongly dependent on the physico-chemical states of the chromate species [3]. This may be influenced by preparation methods. Thus, the effects of the preparation method either co-gel or surface impregnation for the Ti-modified Phillips catalysts were first investigated. Sample **Ph-1** with 2.22 wt.% Ti was prepared by co-gel method, and sample **Ph-2** with similar Ti-loading (2.38 wt.% Ti) was prepared by surface impregnation method. Both of them were similarly treated at 593 °C.

According to our previous reports [16,17], the XPS data obtained within 10 min acquisition of high-resolution scanning could reflect the original physico-chemical nature of surface chromate species (expressed as Cr(VI) $O_{x,surf}$ ) with negligible photo-reduction, and longer XPS acquisition time (over 10 min) could induce photo-reduction of some labile hexa-valent chromate species into tri-valent surface stabilized Cr species (expressed as Cr(III) $O_{x,surf}$ ) due to the soft X-ray irradiation [16,17]. The photo-stability of the chromate species subjected to the soft X-ray irradiation during XPS measurement was further utilized to evaluate the electronic property and polymerization behavior.

The XPS spectra of the Cr 2p core level of the surface chromium species with dependence on XPS acquisition time (10 min, 30 min, and 2 h) for the two samples were presented in Fig. 1. All spectra for **Ph-1** and **Ph-2** were comprised of two main doublet features corresponding to Cr 2p<sub>3/2</sub> and Cr 2p<sub>1/2</sub> photoelectrons, respectively [11]. The individual doublet of each oxidation state was resulted from deconvolution by the peak fitting procedure to estimate the atomic composition of surface chromium species existed in different oxidation states. The specific details relating to the assignments of oxidation states for all surface chromium species based on BE values of Cr 2p<sub>3/2</sub> level of the samples were detailed in our

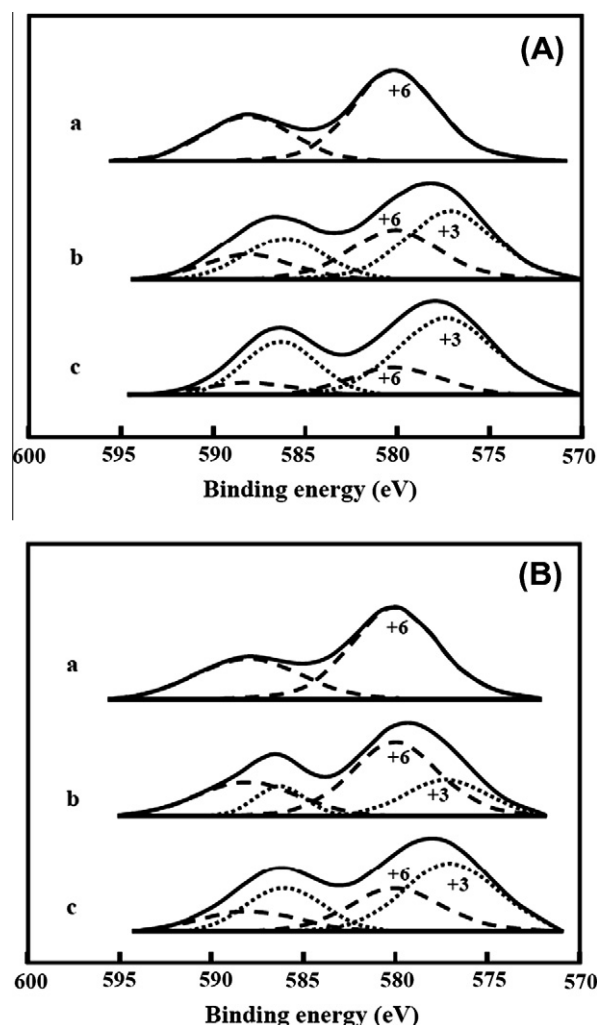


**Fig. 1.** Dependence of XPS spectra of Cr 2p level for catalysts (A) **Ph-1** by co-gel method and (B) **Ph-2** by surface impregnation method on XPS acquisition time: (a) 10 min; (b) 30 min; (c) 2 h.

previous reports [16,17]. For **Ph-1** and **Ph-2** catalysts, the Cr component with BE value of Cr 2p<sub>3/2</sub> level around 580 eV was assigned to be Cr(VI) $O_{x,surf}$  species, and the Cr component with BE value of Cr 2p<sub>3/2</sub> level around 577 eV was assigned to be Cr(III) $O_{x,surf}$  species. Accordingly, the corresponding BE, FWHM values of Cr 2p<sub>3/2</sub> level, assignment and atomic percentage of different oxidation states of surface Cr species were illustrated in Table 2. The 10-

**Table 2**

XPS data from multiplet fitting of Cr 2p spectra with XPS acquisition time within 10 min, 30 min, and 2 h for Ti-modified Phillips catalysts **Ph-1** and **Ph-2** prepared with co-gel and surface impregnation methods, respectively.

Cat.	Temp. (°C)	Ti (wt.%)	XPS				
			Measurement time (min)	BE (eV)	FWHM (eV)	Assignment of Cr species	Cont. (%)
<b>Ph-1</b>	593	2.22	10	580.1	5.4	Cr(VI)	100
			30	580.1	5.7	Cr(VI)	43.1
				577.1	5.7	Cr(III)	56.9
			120	580.1	6.0	Cr(VI)	25.7
				577.3	6.3	Cr(III)	74.3
<b>Ph-2</b>	593	2.36	10	580.0	5.6	Cr(VI)	100
			30	580.0	5.6	Cr(VI)	69.4
				577.2	5.2	Cr(III)	30.6
			120	580.0	5.9	Cr(VI)	38.7
				577.0	6.0	Cr(III)	61.3

min XPS data showed the existence of only a single surface  $\text{Cr(VI)O}_{x,\text{surf}}$  species on **Ph-1** and **Ph-2** catalysts with BE of 580.1 and 580.0 eV and FWHM of 5.4 and 5.6 eV, respectively. Thus, the electronic difference reflected from 10 min XPS data between the samples prepared by the two methods was small. After prolongation of the XPS acquisition time, a new surface  $\text{Cr(III)O}_{x,\text{surf}}$  species appeared on both **Ph-1** and **Ph-2** catalysts due to photo-reduction of  $\text{Cr(VI)O}_{x,\text{surf}}$  species during XPS measurement [16]. It was very interesting to find that the atomic percentage of  $\text{Cr(III)O}_{x,\text{surf}}$  on **Ph-1** of 56.9% (30 min XPS acquisition) and 74.3% (2 h XPS acquisition) were obviously higher than that on **Ph-2** of 30.6% (30 min XPS acquisition) and 61.3% (2 h XPS acquisition) indicating much higher photo-stability of **Ph-2** than that of **Ph-1**. According to our previous report on series of Phillips catalysts calcined at different temperatures (200–800 °C) [16], the catalyst calcined at higher temperatures with higher oxidizing capacity of chromate species and polymerization activity showed better photo-stability of the surface chromate species during XPS measurements. Accordingly, the oxidizing capacity of chromate species and polymerization activity for the **Ph-2** catalyst with a better photo-stability should be higher than that of **Ph-1** with similar Ti-loading. It is reasonable considering a more effective use of the titania by surface impregnation method than that of the co-gel one with partial Ti species in the bulk of silica gel [34], and Ti-modified Phillips catalysts made by surface impregnation method are more popularly used for commercial application. Therefore, the following research was focused on the catalysts prepared by surface impregnation method.

### 3.2. Experimental study of effects of calcination temperature and Ti-loading

Calcination temperature and Ti-loading are crucial factors to determine the catalytic performance of Ti-modified Phillips catalyst. The practical calcination temperature is usually between 500 and 900 °C in industrial processes. Among this temperature region, the thermal-induced reduction of chromate species and catalyst sintering could be negligible. Two series of catalysts calcined at 650 and 820 °C were considered in this work. Three catalysts were calcined at 650 °C: **Ph-3** (Ti-free), **Ph-4** (2.38 wt.% Ti) and **Ph-5** (3.45 wt.% Ti), and another three catalysts were calcined at 820 °C: **Ph-6** (Ti-free), **Ph-7** (2.38 wt.% Ti), and **Ph-8** (3.45 wt.% Ti) with different Ti-loading were characterized by XPS method. Figs. 2 and 3 show the Cr 2p spectra of the six catalysts with dependence of XPS acquisition time from 10 min to 30 min and 2 h. The corresponding BE, FWHM values of Cr  $2p_{3/2}$  level, assignment and atomic percentage of different oxidation states of surface Cr species of each catalyst were illustrated in Table 3. The XPS data obtained at 10-min acquisition time could reflect the original nature of surface chromate species of the catalysts. It was found that only single component of surface chromate species was detected for all the catalysts based on the 10-min XPS data. For **Ph-3**, **Ph-4**, and **Ph-5** catalysts calcined at 650 °C, the BE values of Cr  $2p_{3/2}$  level were 580.6, 580.9 and 581.1 eV, respectively. For **Ph-6**, **Ph-7**, and **Ph-8** catalysts calcined at 820 °C, the BE values of Cr  $2p_{3/2}$  level were 580.8, 581.1 and 581.2 eV, respectively. The slight increase in BE values indicated that the electron-deficiency of surface chromate species increased with increase in Ti-loading. The slight increase in the FWHM values after Ti-modification indicated the broadening of the distribution of surface chromate species. The effect of calcination temperature could be observed from the comparison of the two series of catalysts calcined at 650 °C and 820 °C. When the calcination temperature increased from 650 °C to 820 °C, the BE values of **Ph-3** and **Ph-6** (without Ti-modification) were slightly increased from 580.6 to 580.8 eV, and the corresponding FWHM values broadened from 4.9 to 5.8 eV, respectively. Similar tendency

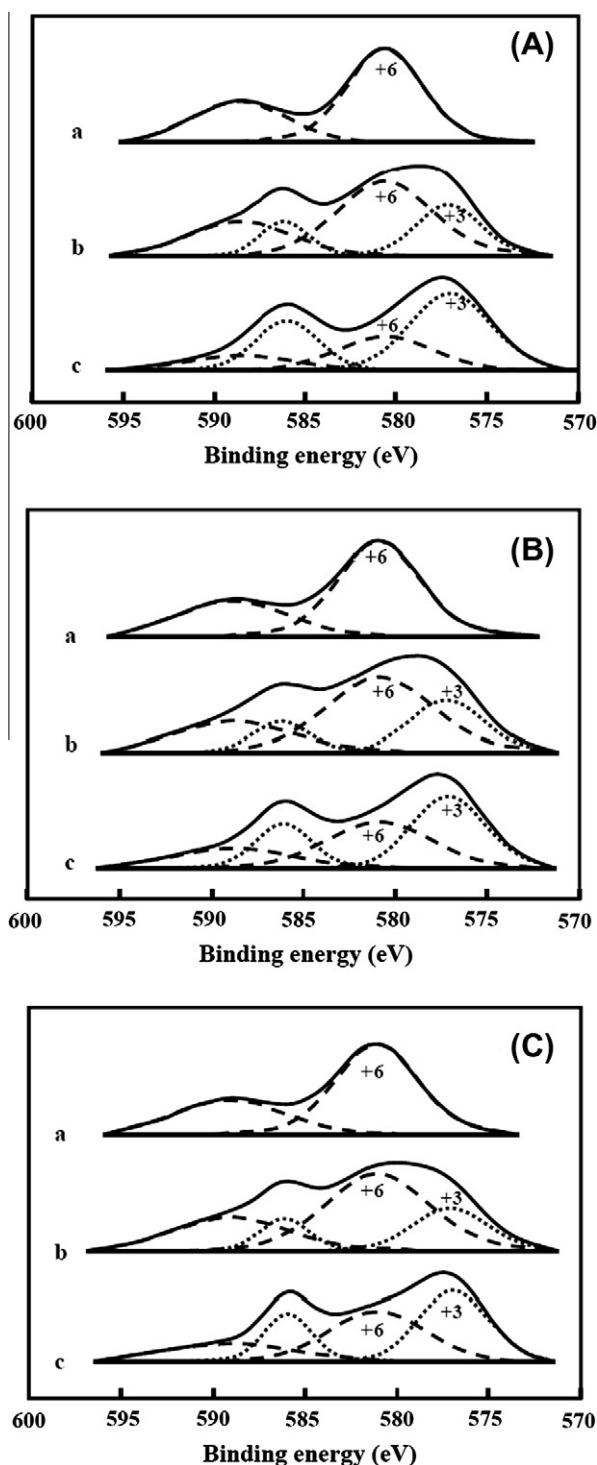
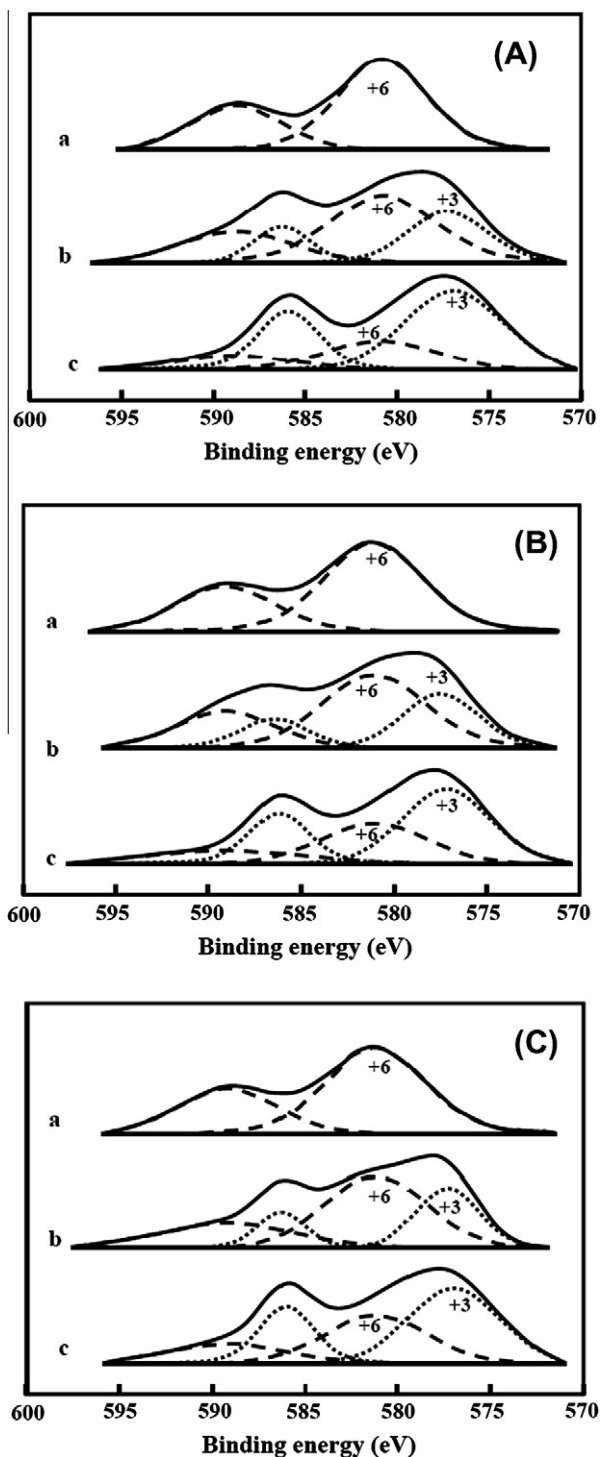


Fig. 2. Dependence of XPS spectra of Cr 2p level for (A) **Ph-3**, (B) **Ph-4** and (C) **Ph-5** catalysts calcined at 650 °C on XPS acquisition time: (a) 10 min; (b) 30 min; (c) 2 h.

was observed between **Ph-4** and **Ph-7** (with 2.38 wt.% Ti, with BE from 580.9 to 581.1 eV, with FWHM from 5.3 to 6.3 eV) and also between **Ph-5** and **Ph-8** (with 3.45 wt.% Ti, with BE from 581.1 to 581.2 eV, with FWHM from 5.3 to 6.3 eV). This means the increase in calcination temperature showed similar effect with increase in Ti-loading in terms of increase in the electron-deficiency of surface chromate species, which could be rationalized by the removal of more electron-donating surface hydroxyl groups and the increase in surface tension due to dehydroxylation at higher calcination temperatures [35].



**Fig. 3.** Dependence of XPS spectra of Cr 2p level for (A) **Ph-6**, (B) **Ph-7**, and (C) **Ph-8** catalysts calcined at 820 °C on XPS acquisition time: (a) 10 min; (b) 30 min; (c) 2 h.

As can be seen from Figs. 2 and 3 and Table 3, when the XPS acquisition time was increased from 10 min to 30 min and 2 h, surface  $\text{Cr(III)}\text{O}_{x,\text{surf}}$  species appeared on all catalysts due to photo-reduction of  $\text{Cr(VI)}\text{O}_{x,\text{surf}}$  species during XPS measurement [16]. The lower amount of  $\text{Cr(III)}\text{O}_{x,\text{surf}}$  species reflected the higher photo-stability of the catalyst. After 30 min XPS acquisition, the Ti-free **Ph-3** catalyst presented a considerable portion of 31.5%  $\text{Cr(III)}\text{O}_{x,\text{surf}}$  species converted from  $\text{Cr(VI)}\text{O}_{x,\text{surf}}$  species then to a dominant portion of 65.3% after 2 h XPS measurement accompa-

nied by a large increase in FWHM from 4.9 up to 6.3 eV. Comparably, for the Ti-modified samples, the corresponding portion of  $\text{Cr(III)}\text{O}_{x,\text{surf}}$  were 31.0% and 28.1% for **Ph-4** and **Ph-5** after 30 min XPS acquisitions and increased to 51.3% and 49.9% after 2 h XPS acquisition, respectively. After 30 min XPS acquisition, the Ti-free **Ph-6** catalyst presented a considerable portion of 35.5%  $\text{Cr(III)}\text{O}_{x,\text{surf}}$  species converted from  $\text{Cr(VI)}\text{O}_{x,\text{surf}}$  species then to a dominant portion of 70.5% after 2 h XPS measurement accompanied by a large increase in FWHM from 5.8 up to 7.1 eV. Comparably, for the Ti-modified samples, the corresponding portion of  $\text{Cr(III)}\text{O}_{x,\text{surf}}$  were 34.5% and 33.9% for **Ph-7** and **Ph-8** after 30 min XPS acquisitions, and increased to 60.5% and 57.6% after 2 h XPS acquisition, respectively. It was very interesting to find that Ti-modification could obviously decrease the amount of the  $\text{Cr(III)}\text{O}_{x,\text{surf}}$  species and thus increase the photo-stability of the Phillips catalysts mainly based on the 2 h XPS data. This was also consistent with the experimental fact of increasing polymerization activity after Ti-modification for Phillips catalysts calcined at the same temperature. However, the mechanism about the increase in photo-stability of Phillips catalyst by Ti-modification was still unclear. It seems contradictory that chromate species with increased electron-deficiency due to the presence of more electronegative Ti(IV) in the neighborhood showed even higher photo-stability during XPS acquisition. Further mechanistic elucidation of the photo-induced reduction of surface chromate species by soft X-ray irradiation during XPS measurement is needed in order to rationalize this point.

As demonstrated above, the gradual shift toward higher BE and FWHM values of Cr  $2p_{3/2}$  level for the surface chromate species in the Ti-modified catalyst with increase in Ti content suggested that the Ti-modification increased the oxidizing capacity of the surface chromate species associated with Ti and thus could shorten the induction period and increase the polymerization activity as well. It is reasonable to suggest the presence of at least two kinds of  $\text{Cr(VI)}\text{O}_{x,\text{surf}}$  species in the Ti-modified catalyst: one species with (Cr–O–Si) neighbors and the other with at least one (Cr–O–Ti) neighbor as shown in Scheme 1. Only those  $\text{Cr(VI)}\text{O}_{x,\text{surf}}$  species with at least one (Cr–O–Ti) neighbor having higher electron-deficiency than that in the Ti-free catalyst may be attributed to the high polymerization activity in experiment, which was confirmed in our DFT calculations, and would be introduced in detail in the following sections. This also coincided with the evidence that 0.5 wt.% Cr on pure titania support was prone to be reduced and formed a large fraction in oxidation state of +5 [36]. And the  $\text{H}_2$ -TPR signal also gave a direct indication of the more easily reducible species in Ti-modified Phillips catalyst [12].

Another powerful tool to detect the effect of Ti-modification on the surface physico-chemical nature is high-resolution  $^1\text{H}$  MAS solid-state NMR. Due to the spectral overlap of Ti–OH and Si–OH, this distinction is very difficult to be obtained by infrared spectroscopy [37]. Fortunately,  $^1\text{H}$  MAS solid-state NMR with high resolution could allow differentiating the Si–OH and the Ti–OH species, yielding thereby useful information on the surface structures on silica gel support modified by titania. Fig. 4A and B presents the  $^1\text{H}$  MAS solid-state NMR signals of **Ph-3**, **Ph-4**, and **Ph-5** catalysts calcined at 650 °C, and **Ph-6**, **Ph-7**, and **Ph-8** samples calcined at 820 °C, respectively. There were three peaks in **Ph-3** spectrum: one main peak near 1.7 ~ 1.8 ppm was assigned to the Si–OH species, and the other two near 9 and –8 ppm were the satellite peaks of the main peak, whose intensities decreased with the decrease in main peak. Similar spectra presented for **Ph-4** and **Ph-5** except a weak band at 6 ppm, which could be attributed to Ti–OH on amorphous but anatase-like titania [38]. Though this was the residual Ti–OH signal after the treatment of the catalyst at high temperatures, it was the first NMR evidence to confirm the existence of the residual Ti–OH groups on the Ti-modified Phillips catalyst.

**Table 3**  
XPS data from multiplet fitting of Cr 2p spectra with XPS acquisition time within 10 min, 30 min, and 2 h for **Ph-3** ~ **Ph-8** Phillips catalysts calcined at different temperatures.

Cat.	Temp. (°C)	Ti (wt.%)	XPS				
			Measurement time (min)	BE (eV)	FWHM (eV)	Assignment of Cr species	Cont. (%)
<b>Ph-3</b>	650	–	10	580.6	4.9	Cr(VI)	100
			30	580.6	6.1	Cr(VI)	68.5
				577.1	4.2	Cr(III)	31.5
			120	580.6	6.3	Cr(VI)	34.7
				577.0	5.3	Cr(III)	65.3
<b>Ph-4</b>	650	2.38	10	580.9	5.3	Cr(VI)	100
			30	580.9	6.8	Cr(VI)	69.0
				577.2	4.7	Cr(III)	31.0
			120	580.9	6.8	Cr(VI)	48.7
				577.1	4.8	Cr(III)	51.3
<b>Ph-5</b>	650	3.45	10	581.1	5.3	Cr(VI)	100
			30	581.1	6.6	Cr(VI)	71.9
				577.1	4.7	Cr(III)	28.1
			120	581.0	6.3	Cr(VI)	50.1
				576.9	4.5	Cr(III)	49.9
<b>Ph-6</b>	820	–	10	580.8	5.8	Cr(VI)	100
			30	580.8	6.9	Cr(VI)	64.5
				577.2	5.0	Cr(III)	35.5
			120	580.8	7.1	Cr(VI)	29.5
				576.9	6.3	Cr(III)	70.5
<b>Ph-7</b>	820	2.38	10	581.1	6.3	Cr(VI)	100
			30	581.1	6.6	Cr(VI)	65.5
				577.5	4.8	Cr(III)	34.5
			120	581.1	6.8	Cr(VI)	39.5
				577.2	5.6	Cr(III)	60.5
<b>Ph-8</b>	820	3.45	10	581.2	6.3	Cr(VI)	100
			30	581.2	6.6	Cr(VI)	66.1
				577.3	4.1	Cr(III)	33.9
			120	581.2	6.5	Cr(VI)	42.4
				577.0	5.8	Cr(III)	57.6

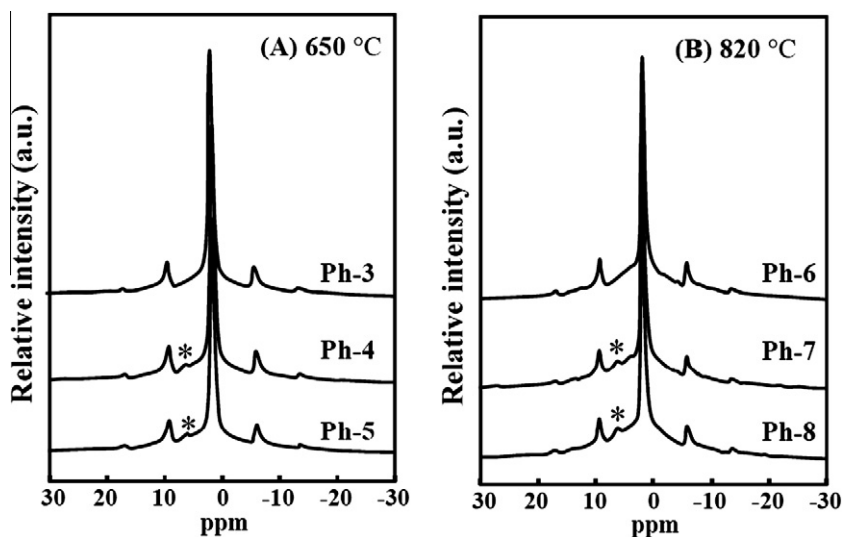


**Fig. 4.**  $^1\text{H}$  MAS solid-state NMR spectra for (A) **Ph-3**, **Ph-4**, and **Ph-5** catalysts calcined at 650 °C, and (B) **Ph-6**, **Ph-7**, and **Ph-8** catalysts calcined at 820 °C. (\*peak of surface Ti–OH groups)

Thus, the surface titania sites might render the Cr site incorporation [2]. The result also indirectly confirmed the reliability of our calculation cluster models with one or two Cr–O–Ti bridges designed for Ti-modified Phillips catalysts. The direct observation of surface residual Ti–OH groups on the **Ph-7** and **Ph-8** catalysts calcined at 820 °C in Fig. 4B were similar to those of their counterparts calcined at 650 °C.

In summary, the high-resolution XPS studies on Ti-modified Phillips catalysts clearly confirmed that Ti-modification led to the increase in electron-deficiency and the photo-stability of the surface chromate species and thus rationalized well the higher oxidizing capacity of chromate species, shorter induction period and higher polymerization activity after Ti-modification. The plausible formation of active Cr species supported on silica gel support



through one or two Cr–O–Ti bridges on Ti-modified Phillips catalysts was further proved by high-resolution  $^1\text{H}$  MAS solid-state NMR method through the first direct evidence of the surface residual Ti–OH groups. These experimental approaches proved the reliability of the catalyst models and provided a solid basis for our theoretical and computational molecular modeling for Ti-modified Phillips catalysts. The basic understanding of Ti-modification on Phillips catalyst solely from experimental approaches is limited at its stronger Brønsted acidity, which could be clearly observed from our  $^1\text{H}$  MAS solid-state NMR characterization. However, as a matter of fact, the unique features for the Ti-modified Phillips catalyst were not entirely derived from the acidity of Brønsted sites in the presence of titania. It is known that many other oxide additives which also enhance Brønsted acidity do not present similar effects [2]. Surely, some other physico-chemical factors may also contribute to the unique performances of Ti-modified Phillips catalyst, which could be possibly elucidated by the following DFT calculations.

### 3.3. Theoretical study of Ti-modification on catalyst activity

Based on the aforementioned experimental investigations, six mononuclear chromium cluster models including three hexavalent  $\text{Cr(VI)}\text{O}_{x,\text{surf}}$  site models (**a0**, **b0**, **c0**) and three divalent  $\text{Cr(II)}\text{O}_{x,\text{surf}}$  site models (**a1**, **b1**, **c1**) with 0, 1 or 2 Cr–O–Ti bridges were utilized to mimic all the possible Ti-modification environments on Phillips catalyst surface (shown in Scheme 2) in our molecular modeling. The effects of Ti-modification on Phillips catalysts with respect to its promotion of polymerization activity, extension of MWD to lower MW region, improvement of the distribution of the inserted co-monomer, and the enhancement of 2,1-insertion in regioselectivity were systematically investigated by DFT method. First, the promotion effect of Ti-modification in terms of polymerization activity enhancement was studied. Activity of Phillips catalyst was mainly determined by several reaction steps in the whole process of polymerization including reduction of  $\text{Cr(VI)}\text{O}_{x,\text{surf}}$  species, chain initiation, and chain propagation, which were calculated with respect to the effects of Ti-modification.

$\text{Cr(VI)}\text{O}_{x,\text{surf}}$  species, which formed during calcination of catalyst, has to be reduced to lower valence state to form Cr active site. Requiring no extra reducing agent like Al–alkyl cocatalyst,  $\text{Cr(VI)}\text{O}_{x,\text{surf}}$  species is considered to be reduced by ethylene monomer to divalent  $\text{Cr(II)}\text{O}_{x,\text{surf}}$ , which has been generally accepted as the final precursor of active site [3,39–41]. All the optimized geometries of ground state for  $\text{Cr(VI)}\text{O}_{x,\text{surf}}$  and  $\text{Cr(II)}\text{O}_{x,\text{surf}}$  models were listed in Table 4. The calculated bond distances  $d(\text{Cr–O})$ , 1.75 Å and 1.75 Å in **a0** were in the same range of 1.706–1.782 Å as that in the synthesized  $\text{CrO}_2(\text{OSiPh}_3)_2$  and  $[\text{CrO}_2(\text{OSiPh}_2)_2\text{O}]_2$  molecules [42,43]. And the bond distance of  $d(\text{Cr–O})$  was also favorably agreed with 1.77 Å in Espelid's work [19] and 1.75 Å in Scott's work [22] based on the same model. Besides, the Cr–O single bond lengths were somewhat lengthened in Ti-involved models, as

1.77 Å, 1.76 Å for **b0**, and 1.77 Å, 1.77 Å for **c0**. Meanwhile, the O–Cr–O bond angle also slightly opened from 104.7° for **a0**, to 105.1° for **b0**, and 106.0° for **c0**. Compared to the **a0** (0 presented the Cr in oxidation of +6) model, Ti-modified models showed an obvious increased Mulliken charges on  $\text{Cr(VI)}$ : +1.11 for **a0**, +1.27, and +1.32 for Ti-modified sites **b0** (Ti:Cr = 1:1) and **c0** (Ti:Cr = 2:1), respectively. The increase in Mulliken charges on the  $\text{Cr(VI)}$  was the direct indication of increase in electron-deficiency of the  $\text{Cr(VI)}$  site with Ti-modification, which facilitated the reduction of chromate species, thereby resulting in a shorter induction period in polymerization process. And this was consistent well with the increase in BE of the surface chromate species after Ti-modification by XPS method as demonstrated in the previous sections.

After the reduction of  $\text{Cr(VI)}\text{O}_{x,\text{surf}}$  species into  $\text{Cr(II)}\text{O}_{x,\text{surf}}$  species, the initiation of the first polymer chain should occur on this  $\text{Cr(II)}$  site triggering the ethylene polymerization. However, the chain initiation step still remains mysterious [1,44–48]. One proposed mechanism of chain initiation involves the direct formation of  $\text{Cr(III)}\text{–ethyl}$  active site from  $\text{Cr(II)}$  site and coordinated ethylene with an extra hydrogen atom. However, the origin of this extra hydrogen atom is postulated from silanol [49] or other surface ligands [3] without reasonable interpretation. In recent years, it is becoming widely accepted that the first polymer chain might be initiated through a metallacyclic mechanism [3,47,50–53]. As shown in Scheme 3, the initiation occurred through the formation of chromacyclopentane five-membered ring from an oxidative coupling reaction between  $\text{Cr(II)}\text{O}_{x,\text{surf}}$  species and two coordinated ethylene molecules, then the first polymer chain grows in loop style by continuous ethylene insertion into the  $\text{Cr(IV)}\text{–C}$  bonds. The results of the formation of chromacyclopentane calculated by DFT were shown in Table 5. The energy barrier of the initiation reaction for **a1**, **b1**, and **c1** models was 6.1, 6.8, and 6.9 kcal mol $^{-1}$ , respectively. The slight increase in the energy barriers suggested that Ti-modification was slightly unfavorable for the initiation reaction. As shown in Table 4, Mulliken charges on  $\text{Cr(II)}$  site were +0.61 for **a1**, +0.90 for **b1**, and +0.77 for **c1**. It is noticeable that the increase in Mulliken charge with the increase in the Ti contents involved in the models was not monotonous. It is likely that the asymmetric structure of the **b2** model led to its much higher Mulliken charge on the  $\text{Cr(II)}$  site. This could be also clearly observed from its structural parameters shown in Table 4. The Cr–O single bonds were 1.78/1.78, 1.85/1.82, 1.78/1.78 Å for **a1**, **b1**, and **c1** models, respectively, and the corresponding O–Cr–O bond angles were 118.7°, 114.6°, and 122.2°, respectively.

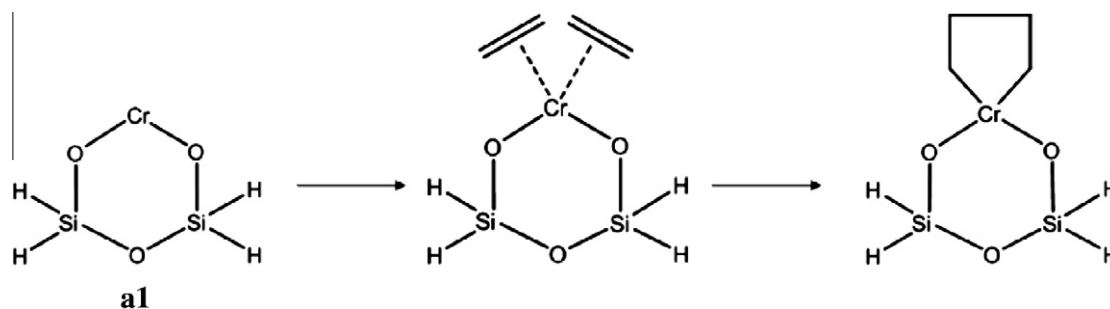
After initiation of the first polymer chain on Phillips catalyst, hundreds of polymer chains would be formed on the same active site during chain propagation step, thus, the chain propagation reactions during this step make more important contribution to the polymerization activity than the initiation reaction. Different with the initiation reaction, the chain propagation from the second polymer chain on each active site is generally considered to follow the classical Cossee mechanism, in which a growing polymer chain propagates in a linear  $\text{Cr}(\text{CH}_2)_n\text{–CH}_3$  pattern with an increase in two methylene units as each coordinated ethylene inserts into the Cr–alkyl bond (as shown as reaction a in Scheme 4) [2,19,44]. In this study, the propagating polymer chain was simplified as a methyl group, thus the Cr–methyl bond was designated as the active site model for continuous insertion of ethylene monomers. The Mulliken charge on Cr active site of the Cr–methyl structures increased from +0.74 for unmodified site model (Ti:Cr = 0:1), to +0.83 for Ti-modified site model (Ti:Cr = 1:1), and +0.89 for Ti-modified site model (Ti:Cr = 2:1), and the corresponding energy barriers of the first ethylene insertion (as shown in Table 5) were 19.2, 18.4, and 17.7 kcal mol $^{-1}$ , respectively. It indicated that the Cr active site became more electron-deficient and thus achieved

**Table 4**

Geometric parameters and Mulliken charges for  $\text{Cr(VI)}$  site models (**a0** for Ti:Cr = 0:1, **b0** for Ti:Cr = 1:1, **c0** for Ti:Cr = 2:1) and  $\text{Cr(II)}$  site models (**a1** for Ti:Cr = 0:1, **b1** for Ti:Cr = 1:1, **c1** for Ti:Cr = 2:1).<sup>a</sup>

Models	Cr–O <sub>1</sub>	Cr–O <sub>2</sub>	O <sub>1</sub> –Cr–O <sub>2</sub>	q(Cr)
<b>a0</b>	1.75	1.75	104.7	+1.11
<b>b0</b>	1.77	1.76	105.1	+1.27
<b>c0</b>	1.77	1.77	106.0	+1.32
<b>a1</b>	1.78	1.78	118.7	+0.61
<b>b1</b>	1.85	1.82	114.6	+0.90
<b>c1</b>	1.78	1.78	122.2	+0.77

<sup>a</sup> Bond length in Å, bond angles in degrees.



**Scheme 3.** Chain initiation over **a1** model through metallacycle mechanism.

**Table 5**

Energy barriers for chain initiation, chain propagation, and chain transfer reactions on various models of Phillips catalysts.<sup>a</sup>

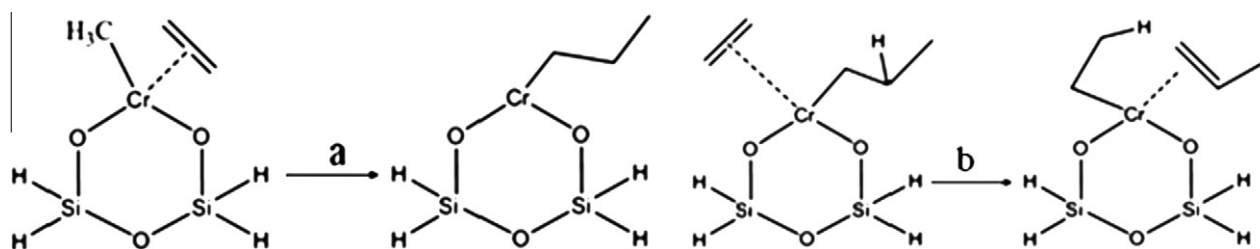
Models	Initiation	Chain propagation <sup>b</sup>			Chain transfer <sup>c</sup>			$\Delta^d$		
	C <sub>2</sub> H <sub>4</sub>	C <sub>2</sub> H <sub>4</sub>	1-C <sub>4</sub> H <sub>8</sub>	1-C <sub>6</sub> H <sub>12</sub>	C <sub>2</sub> H <sub>4</sub>	1-C <sub>4</sub> H <sub>8</sub>	1-C <sub>6</sub> H <sub>12</sub>	C <sub>2</sub> H <sub>4</sub>	1-C <sub>4</sub> H <sub>8</sub>	1-C <sub>6</sub> H <sub>12</sub>
Ti:Cr = 0:1	6.1	19.2	21.7	21.8	25.9	26.1	24.3	6.7	4.4	2.5
Ti:Cr = 1:1	6.8	18.4	20.2	21.2	24.7	23.5	23.3	6.3	3.3	2.1
Ti:Cr = 2:1	6.9	17.7	19.6	20.3	24.1	21.7	22.1	6.4	2.1	1.8

<sup>a</sup> Energy barrier in kcal mol<sup>-1</sup>.

<sup>b</sup> Based on primary 1,2-insertion.

<sup>c</sup> Based on  $\beta$ -H elimination to monomer after 1,2-insertion of the corresponding monomer or co-monomer.

<sup>d</sup> Energy barrier difference between ethylene insertion of chain propagation and chain transfer steps in kcal mol<sup>-1</sup>.



**Scheme 4.** (a) Chain propagation through classical Cossee mechanism and (b) chain transfer by  $\beta$ -H elimination to monomer, for Phillips catalyst.

lower propagation energy barriers due to Ti-modification. The obvious decrease in energy barrier for ethylene insertion during chain propagation indicated that Ti-modification might be one of the main factors bringing the Ti-promotional effects to enhance the polymerization activity of Phillips catalyst.

In summary, the promotional effect of Ti-modification in terms of polymerization activity enhancement was found to be mainly derived from the increase in electron-deficiency of Cr(VI) $O_{x,surf}$  species resulting in the easier reduction into Cr(II) $O_{x,surf}$  species and chain propagation reaction. Ti-modification was found to be slightly unfavorable for the initiation reaction. The increased Mulliken charge on Cr sites involved in Ti-contained Cr(VI), Cr(II) and Cr-methyl active sites provided solid evidences for the fact that electron density of Cr site decreased obviously because of the electron-withdrawing effect of Ti(IV). This was consistent with many experimental reports [2,3,5,10,54].

#### 3.4. Theoretical study of Ti-modification on microstructures of polyethylene chains

According to experimental reports [2,3], Ti-modified Phillips catalysts are known to be able to regulate the microstructures of the polyethylene chains in terms of extension of MWD to lower MW region, improvement of the distribution of inserted co-monomers through decreasing the co-monomer incorporation in the low

MW region. The energetic information about chain transfer for ethylene homo-polymerization, chain propagation, and chain transfer during ethylene copolymerization with  $\alpha$ -olefin was further calculated by DFT method in order to elucidate the specific mechanisms behind the two seemingly contradictory points declared by McDaniel [2]. One was that Ti-modified Cr active sites preferred to produce low MW polyethylene with low co-monomer incorporation, while low MW polyethylene made by Cr active sites without Ti-modification showed high co-monomer incorporation. The other was that the chain transfer response to co-monomer of Ti-modified Phillips catalyst was much greater than that of Ti-free Phillips catalyst, while the product of the Ti-modified Phillips catalyst incorporated much less co-monomer contents.

The MW and MWD of the polyethylene are known to be determined by the relative rate between chain propagation and chain transfer.  $\beta$ -H elimination to monomer is believed to be the predominating chain transfer mode for Phillips catalyst [2]. As for ethylene homo-polymerization, the chain transfer mode was shown as reaction **b** in Scheme 4. According to Table 5, energy barrier of chain transfer was 25.9 kcal mol<sup>-1</sup> for Ti-free model, which was higher than 24.7 and 24.1 kcal mol<sup>-1</sup> for Ti-modified site models of Ti:Cr = 1:1 and Ti:Cr = 2:1, respectively. According to the energy barrier for chain propagation discussed in the previous section, those for chain propagation and chain transfer were simultaneous decreased by Ti-modification, while the later decreased more. This

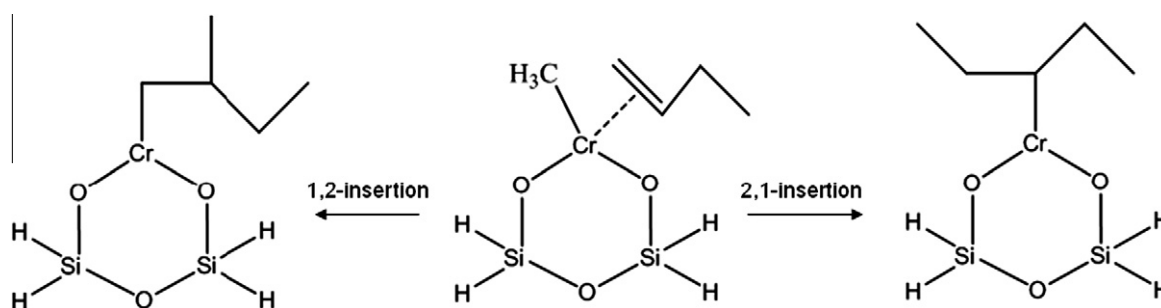
means chain transfer rate was enhanced more than chain propagation rate after Ti-modification. Consequently, Ti-modification would result in an increased low MW fraction of polyethylene, and thus the MWD broadened to the lower MW region. The calculation results provided deeper theoretical understanding on the experimental facts regarding the effects of Ti-modification on the MW and MWD of polyethylene over Phillips catalyst.

Ethylene copolymerization with  $\alpha$ -olefin such as 1-butene or 1-hexene over Phillips catalyst is the key method to control the density and microstructures of the polyethylene products in industrial processes [9]. The dominant primary 1,2-insertions of 1-butene and 1-hexene and subsequent chain transfer by  $\beta$ -hydride elimination to ethylene monomer were investigated by DFT method on the basis of the three type models with 0:1, 1:1, and 2:1 Ti/Cr atomic ratios. The energy data were listed in Table 5 for direct comparison. For the Ti-free catalyst model, the energy barrier of insertion was increased from 19.2 kcal mol<sup>-1</sup> for ethylene, to 21.7 and 21.8 kcal mol<sup>-1</sup> for 1-butene and 1-hexene, respectively, reflecting the general discipline of lower polymerization rate for  $\alpha$ -olefin compared with that for ethylene. For the Ti-modified catalyst models, the energy barrier of 1-butene insertion decreased from 21.7 kcal mol<sup>-1</sup> for Ti-free site model (Ti:Cr = 0:1) to 20.2 and 19.6 kcal mol<sup>-1</sup> for two Ti-modified site models (Ti:Cr = 1:1 and Ti:Cr = 2:1). The energy barrier of 1-hexene insertion also decreased from 21.8 to 21.2 and 20.3 kcal mol<sup>-1</sup> for the Ti-free site model (Ti:Cr = 0:1), and two Ti-modified site models (Ti:Cr = 1:1 and Ti:Cr = 2:1), respectively. It indicates that Ti-modification could promote the activity not only for ethylene homo-polymerization but also for copolymerization with  $\alpha$ -olefins for Phillips catalyst. A comparison between 1-butene and 1-hexene insertions showed the general tendency of lower copolymerization rate for  $\alpha$ -olefin with larger carbon atoms. In order to obtain the distribution of the inserted co-monomers in polyethylene chains [2], the difference in energy barrier between co-monomer insertion and chain transfer, which proceeded with a tertiary  $\beta$ -hydride elimination after the 1-butene or 1-hexene insertion, was also calculated. In Table 5, for the case of 1-butene as co-monomer, the energy barrier difference decreased due to Ti-modification from

4.4 kcal mol<sup>-1</sup> for Ti-free site model (Ti:Cr = 0:1) to 3.3 kcal mol<sup>-1</sup> for Ti-modified site model (Ti:Cr = 1:1) and 2.1 kcal mol<sup>-1</sup> for Ti-modified site model (Ti:Cr = 2:1). Similar tendency was also observed for the case of 1-hexene as co-monomer. The energy barrier difference between 1-hexene 1,2-insertion and subsequent chain transfer decreased due to Ti-modification from 2.5 kcal mol<sup>-1</sup> for Ti-free site model (Ti:Cr = 0:1) to 2.1 kcal mol<sup>-1</sup> for Ti-modified site model (Ti:Cr = 1:1) and 1.8 kcal mol<sup>-1</sup> for Ti-modified site model (Ti:Cr = 2:1). Thus, Ti-modification created an obvious effect to promote chain transfer after co-monomer incorporation. Moreover, insertion of 1-hexene created more dominant effect than that of 1-butene. According to the calculation results in the previous section, Ti-modified catalyst model tended to produce polyethylene with lower MW. Therefore, it was reasonable to conclude that Ti-modified catalyst model tended to make low MW polyethylene with much less co-monomer insertion because the inserted co-monomer mainly led to chain transfer reaction and left the inserted co-monomer at the chain end. As a result, the increased chain termination by co-monomer resulted in less short chain branches (SCBs) in low MW fraction and higher density of the polymer for Ti-modified Phillips catalyst. This lowering of the co-monomer incorporation in the low MW region was highly desirable for improvements of polymer mechanical properties [9]. These molecular modeling results provided wonderful theoretical explanation to the experimental results reported by McDaniel [2,3,10] that larger vinylidene chain ends presented in polymers made by Ti-modified Phillips catalysts and MI response to 1-hexene by Ti-modified Phillips catalyst was much greater than that by Ti-free Phillips catalysts. The results based on the simple theoretical models also rationalized very well the two seemingly contradictory points declared by McDaniel [2].

### 3.5. Theoretical study of Ti-modification on regioselectivity of catalyst

For traditional heterogeneous olefin polymerization catalysts such as Ziegler–Natta and Phillips catalysts, the regioselectivity is usually very high in the form of 1,2-insertion (primary insertion) of  $\alpha$ -olefins. 2,1-insertion (secondary insertion) is not preferential



Scheme 5. Regiospecific insertion of 1-butene as co-monomer in 1,2-orientation and 2,1-orientation for Phillips catalyst.

Table 6

Energy barriers through different regiospecific insertion modes with co-monomers in terms of regioselectivity on various models of Phillips catalysts.<sup>a</sup>

Model	Insertion modes	1-Hexene	$\Delta^b$	1-Butene	$\Delta^b$
Ti:Cr = 0:1	1,2-insertion	21.8	1.9	21.7	2.2
	2,1-insertion	23.7		23.9	
Ti:Cr = 1:1	1,2-insertion	21.2	1.2	20.2	1.2
	2,1-insertion	22.4		21.4	
Ti:Cr = 2:1	1,2-insertion	20.3	1.8	19.6	1.8
	2,1-insertion	22.1		21.4	

<sup>a</sup> Energy barrier in kcal mol<sup>-1</sup>.

<sup>b</sup> Energy barrier difference between 2,1-insertion and 1,2-insertion in kcal mol<sup>-1</sup> for each active site model.

mainly due to steric hindrance. McDaniel [2] suggested that Ti-modification might enhance the 2,1-insertion based on the experimental evidence of increased trans-internal unsaturation chain ends in the polyethylene chains during ethylene copolymerization with 1-hexene on Ti-modified Phillips catalyst. The effect of Ti-modification on the reaction energies of 1,2-insertion and 2,1-insertion of  $\alpha$ -olefins for copolymerization of Phillips catalyst was calculated by DFT method based on the three catalyst models with Ti:Cr atomic ratios of 0:1, 1:1, and 2:1. The regiospecific insertion of 1-butene on the catalyst site model (Ti:Cr = 0:1) was shown in Scheme 5. All the energy barriers of the two insertion modes for both 1-butene and 1-hexene on the three catalyst models were listed in Table 6.

The much lower energy barriers for the co-monomer with 1,2-insertion than that for 2,1-insertion on all the catalyst models suggested the dominant 1,2-insertion with lower steric hindrance was not changed by the Ti-modification. It should be noted that the energy barriers for both 1,2-insertion and 2,1-insertion of co-monomer all decreased after Ti-modification, which is in consistence with the Ti-promotion effect on activity. Moreover, the energy barriers for 2,1-insertion of co-monomer decreased more than that for 1,2-insertion, which could be observed from the lower difference in energy barriers between 1,2-insertion and 2,1-insertion as shown in Table 6. For 1-hexene, the differences in energy barriers between 1,2-insertion and 2,1-insertion were 1.9, 1.2, and 1.8 kcal mol<sup>-1</sup> for Ti-free site model (Ti:Cr = 0:1) and the two Ti-modified site models (Ti:Cr = 1:1 and Ti:Cr = 2:1), respectively. For 1-butene, the differences in energy barriers between 1,2-insertion and 2,1-insertion were 2.2, 1.2, and 1.8 kcal mol<sup>-1</sup> for Ti-free site model (Ti:Cr = 0:1) and the two Ti-modified site models (Ti:Cr = 1:1 and Ti:Cr = 2:1), respectively. The decrease in both the energy barriers of the 2,1-insertion and the difference in energy barriers between 1,2-insertion and 2,1-insertion of co-monomer was a clear indication of the enhancement of 2,1-insertion by Ti-modification on Phillips catalyst. Our theoretical results perfectly validated McDaniel's suggestion of the plausible enhancement of the 2,1-insertion versus 1,2-insertion during ethylene copolymerization with  $\alpha$ -olefin on Ti-modified Phillips catalyst.

#### 4. Conclusions

In this work, the effects of Ti-modification with respect to its promotion of polymerization activity, extension of MWD to lower MW region, improvement of the distribution of the inserted co-monomer, and enhancement of 2,1-insertion in the regioselectivity of Phillips catalysts were systematically investigated by DFT method in combination with experiments using high-resolution XPS and <sup>1</sup>H MAS solid-state NMR characterization. The high-resolution XPS studies on Ti-modified Phillips catalyst clearly demonstrated that Ti-modification led to the increase in electron-deficiency and the photo-stability of the surface chromate species and thus rationalized well the higher oxidizing capacity of chromate species, shorter induction period and higher polymerization activity after Ti-modification. The Ti-modified catalyst by surface impregnation method showed a better photo-stability and possibly better catalytic performance than that by co-gel method with similar Ti-loading. The plausible formation of active Cr species supported on silica gel support through one or two Cr–O–Ti bridges on Ti-modified Phillips catalysts, and the validity of the catalyst models constructed for molecular modeling was further proved by high-resolution <sup>1</sup>H MAS solid-state NMR method through the first direct evidence of the surface residual Ti–OH groups.

As for the theoretical modeling results, first, the promotional effect of Ti-modification in terms of polymerization activity enhancement was found to be mainly derived from the increase

in electron-deficiency of Cr(VI)O<sub>x,surf</sub> species resulting in its easier reduction into Cr(II)O<sub>x,surf</sub> species, and lower energy barrier for the chain propagation reactions, although Ti-modification was found to be slightly unfavorable for the initiation reaction. Second, the energy barriers for chain propagation and chain transfer were simultaneously decreased by Ti-modification, while the later decreased more. This suggested that chain transfer rate was enhanced more than chain propagation rate after Ti-modification. Consequently, Ti-modification could result in an increased low MW fraction of polyethylene, and thus MWD would be broadened to the lower MW region. The difference in energy barrier between co-monomer insertion and subsequent chain transfer decreased due to Ti-modification and created a significant effect to promote chain transfer after co-monomer incorporation. Moreover, insertion of 1-hexene created more dominant effect than that of 1-butene. It was also reasonable to conclude that Ti-modified catalyst model tended to make low MW polyethylene with much less co-monomer insertion because the inserted co-monomer mainly led to chain transfer reaction and left the inserted co-monomer at the chain end. As a result, the increased chain termination by co-monomer resulted in less short chain branches (SCBs) in low MW fraction and higher density of the polymer for Ti-modified Phillips catalyst. Third, the decrease in both the energy barriers of the 2,1-insertion and the difference in energy barriers between 1,2-insertion and 2,1-insertion of co-monomer was a clear indication of the enhancement of 2,1-insertion by Ti-modification on Phillips catalyst, which perfectly validated McDaniel's suggestion of the plausible enhancement of the 2,1-insertion versus 1,2-insertion during ethylene copolymerization with  $\alpha$ -olefin on Ti-modified Phillips catalyst.

The combined spectroscopic and theoretical modeling results, which rationalized the experimental facts well, provided much deeper mechanistic understanding on the Ti-modified Phillips catalysts and a solid basis for further development in this important field.

#### Acknowledgments

The authors thank the financial support by Key Projects in the National Science & Technology Pillar Program during the 11th Five-Year Plan Period (2007BAE50B04) and National Natural Science Foundation of China (20774025), the research program of the State Key Laboratory of Chemical Engineering, Shanghai Pujiang Talent Plan Project (08PJ14032) and the Program of Introducing Talents of Discipline to Universities (B08021), and also the kind donation of the Ti-modified Phillips catalysts from PQ Corporation.

#### Appendix A. Supplementary material

Supplementary data associated with this article can be found, in the online version, at doi:10.1016/j.jcat.2010.05.002.

#### References

- [1] E. Groppo, C. Lamberti, S. Bordiga, G. Spoto, A. Zecchina, *Chem. Rev.* 105 (2005) 115.
- [2] M.P. McDaniel, in: G. Ertl, H. Knozinger, F. Schüth, J. Weitkamp (Eds.), *Handbook of Heterogeneous Catalysis*, Wiley-VCH, Weinheim, 2008, p. 3733.
- [3] M.P. McDaniel, *Adv. Catal.* 33 (1985) 47.
- [4] J.P. Hogan, D.R. Witt, US Patent 3 622 521, to Phillips Petroleum Company, 1971.
- [5] B. Horvath, US Patent 3 625 864, to Phillips Petroleum Company, 1971.
- [6] R.E. Deitz, US Patent 4 119 569, to Phillips Petroleum Company, 1977.
- [7] C.E. Marsden, *Plast. Rubber Compos. Process. Appl.* 21 (1994) 193.
- [8] A. Ellison, T.L. Overton, *J. Chem. Soc., Faraday Trans.* 89 (1993) 4393.
- [9] P.J. Deslauriers, M.P. McDaniel, *J. Polym. Sci. Part A: Polym. Chem.* 45 (2007) 3135.
- [10] M.P. McDaniel, M.B. Welch, M.J. Dreiling, *J. Catal.* 82 (1983) 118.



- [11] J.M. Jehng, I.E. Wachs, B.M. Weckhuysen, R.A. Schoonheydt, J. Chem. Soc., Faraday Trans. 91 (1995) 953.
- [12] A. Ellison, T.L. Overton, J. Mol. Catal. 90 (1994) 81.
- [13] T.J. Pullukat, R.E. Hoff, M. Shida, J. Polym. Sci. Polym. Chem. Ed. 18 (1980) 2857.
- [14] A.B. Gaspar, C.A.C. Perez, L.C. Dieguez, Appl. Surf. Sci. 252 (2005) 939.
- [15] P.C. Thüne, R. Linke, W.J.H. van Gennip, A.M. de Jong, J.W. Niemantsverdriet, J. Phys. Chem. B 105 (2001) 3073.
- [16] Y. Fang, B. Liu, M. Terano, Appl. Catal. A: Gen. 279 (2005) 131.
- [17] B. Liu, M. Terano, J. Mol. Catal. A: Chem. 172 (2001) 227.
- [18] Y. Okamoto, M. Fujii, T. Imanaka, S. Teranishi, Bull. Chem. Soc. Jpn. 49 (1976) 859.
- [19] O. Espelid, K.J. Borve, J. Catal. 195 (2000) 125.
- [20] O. Espelid, K.J. Borve, Catal. Lett. 75 (2001) 49.
- [21] O. Espelid, K.J. Borve, J. Catal. 205 (2002) 366.
- [22] C.A. Demmelmaier, R.E. White, J.A. van Bokhoven, S.L. Scott, J. Catal. 262 (2009) 44.
- [23] A. Damin, J.G. Vitillo, G. Ricchiardi, S. Bordiga, C. Lamberti, E. Groppo, A. Zecchina, J. Phys. Chem. A 113 (2009) 14261.
- [24] R. Schmid, T. Ziegler, Can. J. Chem. 78 (2000) 265.
- [25] B. Liu, Y. Fang, W. Xia, M. Terano, Kinet. Catal. 47 (2006) 234.
- [26] B. Liu, Y. Fang, M. Terano, Mol. Simul. 30 (2004) 963.
- [27] X. Cao, R. Cheng, Z. Liu, L. Wang, Q. Dong, X. He, B. Liu, J. Mol. Catal. A: Chem. 321 (2010) 50.
- [28] T.J. Pullukat, in: M. Terano, T. Shiono (Eds.), Future Technology for Polyolefin and Olefin Polymerization Catalyst, Technology and Education Publisher, Tokyo, 2002, p. 147.
- [29] M.J. Frisch, G.W. Trucks, H.B. Schlegel, G.E. Scuseria, M.A. Robb, J.R. Cheeseman, J.A. Montgomery Jr., T. Vreven, K.N. Kudin, J.C. Burant, J.M. Millam, S.S. Iyengar, J. Tomasi, V. Barone, B. Mennucci, M. Cossi, G. Scalmani, N. Rega, G.A. Petersson, H. Nakatsuji, M. Hada, M. Ehara, K. Toyota, R. Fukuda, J. Hasegawa, M. Ishida, T. Nakajima, Y. Honda, O. Kitao, H. Nakai, M. Klene, X. Li, J.E. Knox, H.P. Hratchian, J.B. Cross, V. Bakken, C. Adamo, J. Jaramillo, R. Gomperts, R.E. Stratmann, O. Yazyev, A.J. Austin, R. Cammi, C. Pomelli, J.W. Ochterski, P.Y. Ayala, K. Morokuma, G.A. Voth, P. Salvador, J.J. Dannenberg, V.G. Zakrzewski, S. Dapprich, A.D. Daniels, M.C. Strain, O. Farkas, D.K. Malick, A.D. Rabuck, K. Raghavachari, J.B. Foresman, J.V. Ortiz, Q. Cui, A.G. Baboul, S. Clifford, J. Cioslowski, B.B. Stefanov, G. Liu, A. Liashenko, P. Piskorz, I. Komaromi, R.L. Martin, D.J. Fox, T. Keith, M.A. Al-Laham, C.Y. Peng, A. Nanayakkara, M. Challacombe, P.M.W. Gill, B. Johnson, W. Chen, M.W. Wong, C. Gonzalez, J.A. Pople, Gaussian 03, Revision E.01, Gaussian, Inc., Wallingford, CT, 2004.
- [30] A.D. Becke, J. Chem. Phys. 98 (1993) 5648.
- [31] W.Y.C. Lee, R.G. Parr, Phys. Rev. B: Condens. Matter 37 (1988) 785.
- [32] P.J. Hay, W.R. Wadt, J. Chem. Phys. 82 (1985) 270.
- [33] C. Gonzalez, H.B. Schlegel, J. Phys. Chem. 94 (1990) 5523.
- [34] S.J. Conway, J.W. Falconer, C.H. Rochester, J. Chem. Soc., Faraday Trans. 85 (1989) 79.
- [35] B. Liu, Y. Fang, M. Terano, J. Mol. Catal. A: Chem. 219 (2004) 165.
- [36] U. Scharf, H. Schneider, A. Baiker, A. Wokaun, J. Catal. 145 (1994) 464.
- [37] E.F. Vansant, P.V.D. Voort, K.C. Vrancken, Stud. Surf. Sci. Catal. 93 (1995) 363.
- [38] S. Haukka, E.L. Lakomaa, A. Root, J. Phys. Chem. 97 (1993) 5085.
- [39] A.B. Gaspar, J.L.F. Brito, L.C. Dieguez, J. Mol. Catal. A: Chem. 203 (2003) 251.
- [40] A.B. Gaspar, L.C. Dieguez, Appl. Catal. A: Gen. 227 (2002) 241.
- [41] B. Liu, P. Sindelar, Y. Fang, K. Hasebe, M. Terano, J. Mol. Catal. A: Chem. 238 (2005) 142.
- [42] L.M. Baker, W.L. Carrick, J. Org. Chem. 35 (1970) 774.
- [43] H.C.L. Abbenhuis, M.L.W. Vorstenbosch, R.A. van Santen, W.J.J. Smeets, A.L. Spek, Inorg. Chem. 36 (1997) 6431.
- [44] P. Cossee, J. Catal. 3 (1964) 80.
- [45] J.P. Hogan, J. Polym. Sci. Part A–1: Polym. Chem. 8 (1970) 2637.
- [46] L.M. Baker, W.L. Carrick, J. Org. Chem. 33 (1968) 616.
- [47] K.Y. Choi, S. Tang, J. Appl. Polym. Sci. 91 (2004) 2923.
- [48] H.L. Krauss, J. Mol. Catal. 46 (1988) 97.
- [49] P.P.M.M. Wittgen, C. Groeneveld, P.J.C.J.M. Zwaans, H.J.B. Morgenstern, A.H. Van Heugten, C.J.M. Van Heumen, G.C.A. Schuit, J. Catal. 77 (1982) 360.
- [50] V.J. Ruddick, J.P.S. Badyal, J. Phys. Chem. B 102 (1998) 2991.
- [51] E. Groppo, C. Lamberti, S. Bordiga, G. Spoto, A. Zecchina, J. Catal. 240 (2006) 172.
- [52] B. Rebenstorf, R. Larsson, J. Mol. Catal. 11 (1981) 247.
- [53] A. Zecchina, G. Spoto, G. Ghiotti, E. Garrone, J. Mol. Catal. 86 (1994) 423.
- [54] B. Rebenstorf, T. Sheng, Langmuir 7 (1991) 2160.